



Received on 15 April 2023; received in revised form, 12 June 2023; accepted 04 July 2023; published 01 December 2023

IDENTIFYING TUBULIN AS A NEW TARGET OF A DIHYDROPYRIDINE DERIVATIVE, AMLODIPINE BESYLATE

Sampurna Bhattacharya¹, Ansuman Lahiri¹, Suvroma Gupta² and Runa Sur^{* 1}

Department of Biophysics¹, Molecular Biology and Bioinformatics, 92 A. P. C. Road, University of Calcutta - 700009, Kolkata, India.

Department of Biotechnology², Haldia Institute of Technology, ICARE Complex, HIT Campus, Haldia, West Bengal - 721657, Purba Medinipur, India.

Keywords:

Tubulin, Dihydropyridine derivative, Amlodipine besylate, Anti-cancer, AutoDock Vina, Drug repurposing HPMC E50 LV, Pluronic F-127

Correspondence to Author:

Runa Sur

Assistant Professor,
Department of Biophysics,
Molecular Biology and Bioinformatics,
92 A. P. C. Road, University of Calcutta -
700009, Kolkata, India.

E-mail: rsbmbg@caluniv.ac.in

ABSTRACT: The quest for new antimetabolic drugs is an ongoing process where microtubules act as an attractive target for anti-cancer drugs. In this work, we report on the anti-cancer activity of Amlodipine besylate (AB), a salt derivative of the dihydropyridine group drug Amlodipine, a long-acting third-generation calcium channel blocker. Cytotoxicity assay revealed that AB demonstrated cytotoxic effects against cancer cells with greater specificity against cervical cancer cells (IC₅₀ 10 μM) whereas the non-cancerous NKE cells remained unaffected at this dose. AB inhibited HeLa cell migration as observed via scratch assay. Docking studies indicated that AB has the highest binding affinity for vinca site compared to Tubulin's taxol, colchicine, and laulilamide binding domains. AB similarly interacted with tubulin to vinca and established two hydrophobic interactions with VAL³⁵³, PRO³²⁵; hydrogen bonds with ASN³²⁹, VAL¹⁷⁵ and THR²¹⁸ at the binding pocket. The stability of the Tubulin-AB complex was analyzed by molecular simulation studies. Further AB treated cells revealed altered microtubule architecture and drug-induced microtubule depolymerization in HeLa cells. More detailed study might unravel additional binding attributes of AB related to its antimetabolic potential imparting valuable addition to the repurposing of existing medicines.

INTRODUCTION: Drug repurposing is using clinically approved drugs for new applications. A repurposed drug is safe, has proven bioavailability, and is advantageous for drug development¹. The cost and time consumption for developing repurposed drugs is lower compared to *de novo* drug development². Various data and experimental approaches have been developed to repurpose known drugs and successful results have been observed for drugs like Nelfinavir, used for treating

HIV, is in phase I trials for treating solid tumors³. Rapamycin, an immunosuppressant for preventing kidney transplant rejection also acts as mTOR protein inhibitor in signaling pathways for cancer⁴.

Despite advancements in the drug treatment strategies, cancer is still one of the most dreadful diseases worldwide⁵ because of drug resistance, inactivation of drug, apoptosis suppression, altered drug metabolism, enhanced DNA repair and gene amplification leading to multidrug resistance (MDR)⁶. Targeting cytoskeleton proteins is one of the key mechanisms underlying cancer therapy drugs⁷. Microtubules consisting of α and β tubulin dimers are highly dynamic cytoskeletal structures pivotal to mitosis and cell division⁸. Cancer cells divide rapidly by mitosis. These cells rely on proper microtubule assembly to function during

<p>QUICK RESPONSE CODE</p> 	<p>DOI: 10.13040/IJPSR.0975-8232.14(12).5687-00</p> <hr/> <p>This article can be accessed online on www.ijpsr.com</p> <hr/> <p>DOI link: https://doi.org/10.13040/IJPSR.0975-8232.14(12).5687-00</p>
---	--

mitosis. This is the reason why these microtubule epimers act as important targets in anti-cancer drug therapy. Drugs targeting microtubules have been considered effective in treating hematological malignancies and solid tumors. These drugs are known as “microtubule targeting agents” (MTAs). Recent cryo-electron microscopy (cryoEM) advances have shown six different microtubule binding sites for MTAs. Different agents such as Taxane/ Colchicine/ Laulilamide/ Vinca and Maytansine bind to the β tubulin subunit. The only site that resides on α tubulin is the Pironetin binding site⁹. Drugs that bind to the laulilamide site and the taxane/epithilone site acts as tubulin stabilizing agents whereas those that bind to the colchicine site and the vinca alkaloid site acts as destabilizing agents, as evident from past literature¹⁰. The vinblastine or vincristine binding site acts as an important binding domain for compounds that have the potential to depolymerize tubulin¹¹. The synthetic derivatives of vinblastine such as vinorelbine or nor-anhydrovinblastine are widely used in chemotherapeutic treatments¹². Vinblastine binds to the interface of $\alpha\beta$ -tubulin and hampers the normal microtubule function¹³.

Calcium channel blockers (CCBs) are widely used as a first line antihypertensive drug. Depending on the chemical structure, CCBs are categorized into 3 subgroups; benzothiazepines, phenylalkylamines and dihydropyridines (e.g. Amlodipine). 1, 4-Dihydropyridine nucleus acts as an important structure that aids in the interaction of such drugs with diverse receptors¹⁴. The dihydropyridine group is also further clinically classified as 1st, 2nd and 3rd generation drugs on the basis of the structural formula and the length and specificity of action. Amlodipine besylate is a synthetic derivative of Amlodipine, a 3rd generation, L-type CCB belonging to the dihydropyridine group. AB is a salt (besylate) derivative of amlodipine that shares the same basic structure but it has a better drug delivery system as this salt form improves the absorbability of the drug with increased tolerability in patients¹⁵. So, AB is the drug of our interest since it is along-acting drug that has a long half-life with longer retention in the blood. Various reports suggest the repurposing of different CCBs as anti-cancer agents. In the early 1980s, CCBs were found to be inhibitors of multidrug resistance (MDR) in leukemia cells. Verapamil is one such compound

that showed efficacy in reversing MDR¹⁶. A novel Dihydropyridine derivative VdiE-2N acts as an anti-cancer agent by inducing apoptosis in head and neck squamous cell carcinoma cells¹⁷. Lercanidipine, a Dihydropyridine drug exerts its anticancer effect by modulating the T cells¹⁸. Preclinical studies showed that many CCBs had anti-cancer effects but no studies had been done till date to find out whether Dihydropyridine group of drugs could act as microtubule targeting agents (MTAs). The major drawback of chemotherapy is MDR in different types of cancer. So, there is always a need for new drugs to overcome this challenge. Synchronizing with this basic concept of drug repurposing, in our present study we report for the first time, the importance of the basic structure of Amlodipine using its derivative, AB as a potential anti-cancer agent that targets tubulin.

MATERIALS AND METHODS:

Materials: Amlodipine besylate (A5605) and Hoechst 33258 (Sigma-Aldrich), Dulbecco's modified eagle medium (DMEM) and Trypan blue solution (Invitrogen), Penicillin-streptomycin and Trypsin-EDTA(HiMedia), Foetal bovine serum (Gibco), Anti- α -tubulin antibody (BioBharati Life Science Pvt. Ltd), Alexa fluor 568 anti-mouse IgG antibody (Thermofischer scientific).

Molecular Docking and Analysis:

Software and Program: Open Babel GUI version 3.1.1 by Chris Morley was used to convert.SDF file of ligand to .PDB file, PyMol (Delano Scientific LLC, Palo Alto, California, USA), and Discovery Studio Biovia 2020 (Dassault Systèmes, San Diego, California, USA) were used to visualize and modify receptor and ligand structures.

The docking program used in this study was Autodock-Vina (The Scripps Research Institute, La Jolla, San Diego, USA).AutoDock Tools version 1.5.6 (ADT; The Scripps Research Institute, La Jolla, San Diego, USA) was used to prepare the ligand. PDBQT files and Tubulin crystal without inhibitors (colchicine, taxol, vinblastine and laulilamide).PDBQT files and also to determine the grid box size.

Preparation of ligand structure for Amlodipine Besylate and Cevipabulin: Structure of the ligands were downloaded in the Spatial Data file

(.SDF) file format from PubChem Compound Database (National Center for Biotechnology Information; <https://pubchem.ncbi.nlm.nih.gov/>). Chemical structure in the SDF format was converted to the .PDB format using Open Babel. ADT was then used to add rotatable bonds and to convert the ligand .PDB file to .PDBQT file.

Preparation of Protein Structure Tubulin: From the RCSB protein data bank (<http://www.rcsb.org/>), the crystal structure of Tubulin-colchicine complex (1SA0), Tubulin-taxol complex (1JFF), Tubulin-vinblastine complex (1Z2B) and Tubulin-laulilamide complex (4O4H) were downloaded. As the downloaded crystal structure complexes had missing amino acid residues, they were homology modelled using SWISS MODEL tool using as template the crystal structure of 1SA0, 1JFF, 1Z2B and 4O4H. The quality of the models were assessed using GMQE (Global Model Quality Estimation) and QMEAN scoring functions. The GMQE values lie between 0 and 1 and QMEAN score of less than -4 indicate low quality models. The models were also validated by quality structure assessment tool such as PROCHECK. The inhibitors from the best modelled protein structures were then separated using Discovery Studio and saved as separate .PDB file of the inhibitors. Using ADT software, the water molecules were removed, polar hydrogens were added, Kollman charges and Gasteiger charges were added to protein structures and then the .PDB files were converted to .PDBQT files.

Docking Methodology using AutoDock-Vina: Amlodipine besylate was docked to four different inhibitor binding sites of modelled tubulin heterodimer individually. The ligand was flexible and the receptors were rigid. The grid spacing was 0.375 Å. The ligand binding affinity to different Tubulin-inhibitor binding sites were predicted as negative Gibbs free energy (ΔG) scores (kcal/mol), as calculated by AutoDock-Vina. The inhibitor binding site which showed highest affinity for the ligand was chosen for further analysis. The affinity of our drug Amlodipine besylate was then compared to a known compound which was already established as the binding site inhibitor of the domain that showed highest affinity for our ligand. The results were analyzed using PyMol and Discovery Studio Biovia 2020, that showed the binding locations, hydrogen bonds, hydrophobic

interactions and bonding distances. Validation of the docking protocol was done by re-docking co-crystallized ligand in the active sites of Tubulin-colchicine, Tubulin-taxol, Tubulin-vinblastine and Tubulin-laulilamide protein receptors. The docking protocol was validated by the interactions of similar amino acid residues of the re-docked co-crystallized ligand and the native crystal ligand in the active site of the protein.

Molecular Simulations: Molecular dynamics simulations of the protein-ligand complex were carried out using GROMACS version 2021.1. The force field parameters for AB were generated using the SwissParam webserver (<https://www.swissparam.ch/>)²⁶. For the protein part, the GROMACS port of the CHARMM36 force field was used (July 2021 update). The initial structure of the complex was the homology modeled structure based on 1Z2B with docked AB. The complex was solvated in a dodecahedral box of TIP3P water molecules²⁷ with Na⁺ and Cl⁻ ions added to neutralize the complex and the salt concentration was fixed at 0.1 M. The minimum distance of the walls of the solvent box from the solute atoms was kept at 1 nm. To remove short contacts, 50000 steps of steepest descent energy minimization were carried out. The protein ligand complex was restrained using the default force constant. Initially, an NVT simulation was carried out for 100 ps to equilibrate the system at 300 K. The particle mesh Ewald method²⁸ was used for electrostatics and a cut-off of 1.2 nm was used for both non-bonded interactions. Subsequently 100 ps of NPT simulation was carried out to equilibrate the pressure at 1 bar. Finally, the restraints were removed and 4 ns of NPT simulation was carried out for collecting the trajectory for analyses.

Cell Line and Culture Conditions: Human normal kidney epithelial NKE cells, human cervical cancer HeLa cells, human breast cancer MCF-7 cells and human colorectal cancer HCT116 cells were cultured in Dulbecco's modified Eagle medium (DMEM) supplemented with 10% fetal bovine serum (FBS), 100 U/ml penicillin and 100 mg/ml streptomycin at 37°C and 5% CO₂. Then, HeLa/MCF-7/HCT116/NKE cells were grown in the absence or presence of different concentrations of drugs (dissolved in DMSO) for 24 hours, the final concentration of DMSO was 0.05% of the

total volume. The effects of Amlodipine besylate on cell proliferation was determined using established assay methods.

Estimation of Cytotoxicity of Amlodipine Besylate by Trypan Blue Assay: The cytotoxic action of the compound was assayed using Trypan blue on HeLa and normal kidney epithelial (NKE) cells.

In brief, cells were plated at a density of 1×10^5 cells per well for 24 h in 24 well plates and were treated with Amlodipine besylate at varying concentrations for 24 hours. 1:1 ratio of cell suspension and trypan blue solution (0.4%) was added and a hemocytometer count of the population of viable cells was determined for the different doses of the drug. The percentage of viable cells were then determined and plotted.

Scratch Assay: HeLa cells were grown (3×10^5 cells per well) for 24 h in a 6 well plate. When the cells were confluent, a scratch was made using a 200 μ l sterile micropipette in each well. The detached cells were removed by PBS wash. The cells were treated with 10 μ M (IC_{50}) AB concentration for 24 h and 48 h. The cell migration was photographed by an inverted microscope. The experiments were performed in triplicate.

Confocal Microscopy: The effects of Dihydropyridine group of drugs on microtubules were tested by fluorescence microscopy. Briefly, HeLa cells were grown in the presence or absence of Amlodipine besylate for 24 hours on poly-lysine coated glass cover slips. 4% formaldehyde was used to fix the cells which were permeabilized with ice cold ethanol. Blocking was done with 2% BSA in PBS and incubated with mouse monoclonal anti- α -tubulin antibody (1:300 dilution) for 24 hours at 4°C followed by incubation with 1:350 dilution of Alexa-568-labeled anti-mouse IgG antibody for 1 hour. Cells were washed three times with PBST. Nuclear staining was carried out with Hoechst 33258 (0.5 μ g/mL) for 5 min in the dark, washed with PBST once and lastly with PBS. The cover slips were observed under microscope after mounting with Fluomount (Sigma). The microscopy images were generated using a Confocal Microscope (AOBS TCS-SP2 LEICA, GERMANY, Bose Institute central facility).

Determination of the Amount of Soluble and Polymeric Tubulin in Cervical Cells after Amlodipine Besylate Treatment by Western Blot Analysis: HeLa cells were grown in a 6 well plate at 3×10^5 cells per well. After reaching 70% confluency, the cells were incubated in the presence and absence of 10 μ M drug for 24h and 48h. At first the cell pellet was collected and PEM buffer with 25% glycerol and 0.5% triton X-100 was added without disturbing the pellet. It was then incubated for 2min at 37°C and the supernatant was gently removed from the top of the pellet. The supernatant represents the soluble (free) fraction of tubulin. The cell pellet was lysed using Tris-Cl 20Mm (pH-6.8), NaCl 200mM, Triton-X-100 0.1%, DTT 1mM at pH-7.2 for 1h at 4°C. Then it was centrifuged at 13000g for 10 min at 4°C, and the supernatant that consists of polymeric tubulin was collected. The protein concentration was measured using Bradford's assay. Protein from both the soluble and polymeric fraction was analyzed by western blotting using α -Tubulin monoclonal antibody (BioBharati) and the intensity of the bands were analyzed by ImageJ software.

Statistical Analysis: Data were expressed as mean \pm SD and represented at least three independent experiments. P value of < 0.05 was considered to be significant. Student's test was used to obtain differences between groups using KyPlot version 6.0.2.

RESULTS AND DISCUSSION:

Homology Modelling of Tubulin-inhibitor Complexes and Model Validation: The downloaded crystal structure of Tubulin-colchicine (1SA0), Tubulin-taxol (1JFF), Tubulin-vinblastine (1Z2B) and Tubulin-laulilamide (4O4H) complexes were used as templates for developing the homology models of the above crystal structures that had missing amino acid residues using SWISS-MODEL server. The models were scored using GMQE (Global Model Quality Estimate) and QMEAN scoring functions. The GMQE is a coverage-dependent score concerning the alignment between template-target sequence and the QMEAN score is not coverage dependent and is a global score that ensures the global model quality, which should always lie between 0 to 1 for a high-quality model.

PDB ID: 1SA0 and 4O4H have similarity of 87%, 1Z2B has similarity of 80% and 1JFF has 67% similarity between the alignment of the template and target sequence. The QMEAN score obtained from all the models were between 0 to 1 **Table 1**. To ensure the reliability of the models for further carrying out molecular docking simulations, the quality of the models was assessed by online quality structure assessment tool such as PROCHECK software via the Ramachandran Plot along with the Ramachandran plot statistics and the results were compared with their respective Tubulin-inhibitor crystal structures. The Ramachandran plot statistics provide information

regarding the total number of amino acid residues found in the model's favorable, allowed and disallowed region. The statistics provide an idea on the structural reliability of the models generated. The resulting Ramachandran plot statistics are shown in **Table 2**.

TABLE 1: QMEAN AND GMQE SCORE OF THE MODELS GENERATED BY SWISS MODEL

Tubulin-inhibitor crystal structures	QMEAN	GMQE
Tubulin-Colchicine (1SA0)	0.8	0.87
Tubulin-Taxol (1JFF)	0.62	0.67
Tubulin-Vinblastine (1Z2B)	0.74	0.8
Tubulin-Laulilamide (4O4H)	0.81	0.87

TABLE 2: RAMACHANDRAN PLOT STATISTICS OF THE MODELLED CRYSTAL STRUCTURES OBTAINED USING PROCHECK SOFTWARE (M DENOTES MODEL GENERATED BY SWISS DOCK SOFTWARE)

Amino acid residue (%)	1SA0	1SA0_M	1JFF	1JFF_M	1Z2B	1Z2B_M	4O4H	4O4H_M
Most favored regions	74.50	93.60	61.40	75.40	73.40	83.60	91.50	93.60
Additionally allowed regions	19.60	5.70	34.20	16.2	20.80	12.60	8.10	6.20
Generously allowed regions	4.20	0.40	3.60	4.7	3.90	2.00	0.30	0.00
Disallowed regions	1.60	0.20	0.80	3.7	2.00	1.70	0.20	0.20

Molecular Docking revealed that Amlodipine Besylate and Tubulin Interacts at Residue Level in the Vinblastine Binding Site of the Modelled Tubulin-vinblastine Complex (PDB ID:1Z2B):

We used an open source software AutoDock Vina for protein-ligand Docking since it has better accuracy and is a better molecular docking program that can be implemented for accurate binding mode prediction¹⁸ and characterized the interaction of the ligand, a Dihydropyridine derivative (Amlodipine besylate) with the protein Tubulin. In this study, the native ligand was VLB (2 Alpha, 2' Beta, 3 Beta, 4 Alpha, 5 Beta-Vincalculoblastine). **Fig. 1A** showed the model of interaction between VLB and its binding site in tubulin. The amino

acids involved in forming hydrogen and hydrophobic bonds are shown in **Table 3**. The Docking was considered successful when both of the ligands (native ligand and its docked pose) interacted with the same amino acid residues of tubulin i.e. ASP177 (B chain), VAL175 (B chain), THR218 (B chain), TYR208 (B chain) and ASN329 (C chain), PHE351 (C chain), VAL353 (C chain), PRO325 (C chain), VAL328 (C chain), VAL353 (C chain), ILE355 (C chain) **Fig. 1B**. The RMSD between the re-docked co-crystallized ligand and the co-crystallized ligand was less than 2Å, so this docking method could be used to perform the docking calculation of Amlodipine besylate.

TABLE 3: THE INTERACTING RESIDUES OF THE MODELLED TUBULIN-VINBLASTINE CRYSTAL STRUCTURE (PDB ID: 1Z2B) WITH THE CRYSTAL LIGAND VLB AND THE TYPE OF BONDS WITH RESPECTIVE DISTANCES AS VISUALIZED BY DISCOVERY STUDIO BIOVIA 2020. (C DENOTES A CHAIN AND B DENOTES B CHAIN)

Interacting residues	Bond type	Distance (Å)
C:ASN329	Hydrogen Bond	2.89
C:ASN329	Hydrogen Bond	2.67
B:PRO220	Hydrogen Bond	2.78
B:PRO220	Hydrogen Bond	3.34
B:VAL175	Hydrogen Bond	2.76
B:THR218	Hydrogen Bond	3.56
B:ASP177	Hydrogen Bond	3.51
C:PHE351	Hydrogen Bond	3.17
B:TYR208	Hydrogen Bond	3.17
B:TYR208	Hydrogen Bond	2.94
C:ASN329	Hydrogen Bond	4.02

C:ILE332	Hydrophobic	4.77
C:VAL353	Hydrophobic	5.34
B:VAL175	Hydrophobic	4.15
B:VAL175	Hydrophobic	3.69
B:PRO220	Hydrophobic	5.03
B:LEU225	Hydrophobic	4.44
C:PRO220	Hydrophobic	4.21
C:PRO220	Hydrophobic	4.90
B:LYS174	Hydrophobic	3.59
B:PRO220	Hydrophobic	4.89
B:TYR208	Hydrophobic	4.28
B:TYR208	Hydrophobic	4.59
B:PHE212	Hydrophobic	4.66
B:TYR222	Hydrophobic	4.32
C:PRO325	Hydrophobic	4.03
C:VAL328	Hydrophobic	4.62
C:VAL353	Hydrophobic	4.09
C:ILE355	Hydrophobic	5.44
C:VAL353	Hydrophobic	5.43
C:PRO325	Hydrophobic	4.15

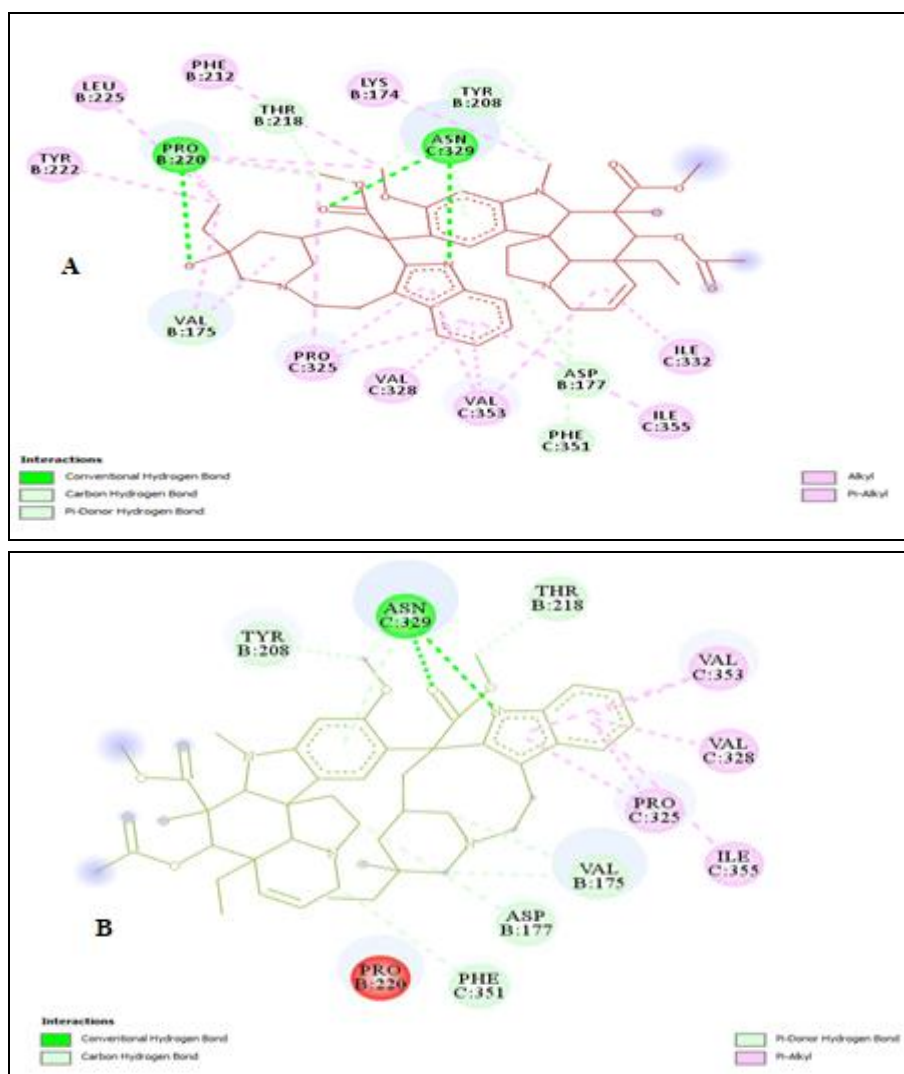


FIG. 1: RESIDUE LEVEL INTERACTION OF A) NATIVE LIGAND VLB (PURPLE) WITH MODELLED TUBULIN-VINBLASTINE COMPLEX (PDB ID: 1Z2B) B) THE BEST DOCKED POSE OF NATIVE LIGAND (GREEN) WITH MODELLED TUBULIN-VINBLASTINE COMPLEX (PDB ID: 1Z2B) OBTAINED FROM DOCKING BY AUTODOCK-VINA AND VISUALIZED BY DISCOVERY STUDIO BIOVIA 2020

Spontaneous binding of the ligand with targeted protein occurs only when the change in free energy is negative. The ΔG values provided information about the docked ligand in the active site pocket which was previously known from the X-ray crystallographic structural information. Docking of

Amlodipine besylate with microtubule showed that at the lowest (1st) conformation it had a ΔG score of -6.0 kcal/mol in the colchicine binding site, -5.7 kcal/mol at the taxol binding site, -6.4 kcal/mol at the vinblastine binding site **Table 4** and -5.6 kcal/mol at the laulilamide binding site **Fig. 2**.

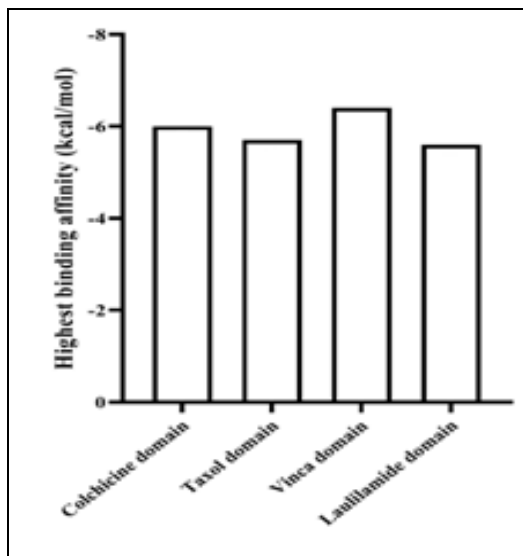


FIG. 2: HIGHEST BINDING AFFINITY OF AMLODIPINE BESYLATE TO DIFFERENT MICROTUBULE INHIBITOR BINDING SITES ON TUBULIN

Besylate has greatest affinity towards the vinblastine binding site with a ΔG score of -6.4 kcal/mol with modelled Tubulin-vinblastine complex (PDB ID: 1Z2B) after docking the ligand using ADT 1.5.6.

The other modelled crystal structures that were used are Tubulin-taxol complex (PDB ID: 1JFF), Tubulin-colchicine complex (PDB ID: 1SA0) and Tubulin-laulilamide complex (PDB ID: 4O4H).

TABLE 4 BINDING AFFINITY OF AMLODIPINE BESYLATE TO THE VINBLASTINE BINDING DOMAIN OF THE MODELLED CRYSTAL TUBULIN-VINBLASTINE COMPLEX (PDB ID: 1Z2B) USING AUTODOCK-VINA: THE DIFFERENT BINDING POSES OF THE LIGAND WITH ITS RESPECTIVE RMSD VALUE SHOWED THAT THE 1ST POSE IS TO BE CONSIDERED AS IT HAS THE HIGHEST BINDING AFFINITY OF -6.4 KCAL/MOL AND RMSD VALUE 0.

Number of docked poses	Binding affinity (kcal/mol)	RMSD (lower bound)	RMSD (upper bound)
1.	-6.4	0	0
2.	-6.4	2.471	6.275
3.	-6.4	2.512	6.164
4.	-6.3	2.877	5.672
5.	-6.3	3.728	7.327
6.	-6.2	3.576	6.513
7.	-6.2	3.023	5.869
8.	-6.2	2.761	6.538
9.	-6.1	2.946	5.632

Vinblastine binding domain is a very important target for identifying drugs for anti-cancer therapy. The main drawbacks of using colchicine group of drugs for cancer therapy is its cytotoxic effects on cells producing hemorrhage and necrosis¹⁹. Numerous drugs have shown their capability of acting as a vinblastine binding site inhibitor and

Cevipabulin is one such drug which has completed clinical trials²⁰. Recent studies indicate that Cevipabulin can bind simultaneously on α -Tubulin (the seventh site) as well as on the vinblastine site²¹. So, we docked Cevipabulin to the modelled tubulin-vinblastine binding site of crystal structure PDB ID: 1Z2B and we found that Amlodipine

besylate has comparable binding affinity of -6.4 kcal/mol to Cevipabulin which revealed the binding affinity of -7.4 kcal/mol **Fig. 3A** and they shared

similar active binding site like the native ligand VLB in the Tubulin-vinblastine complex **Fig. 3B**.

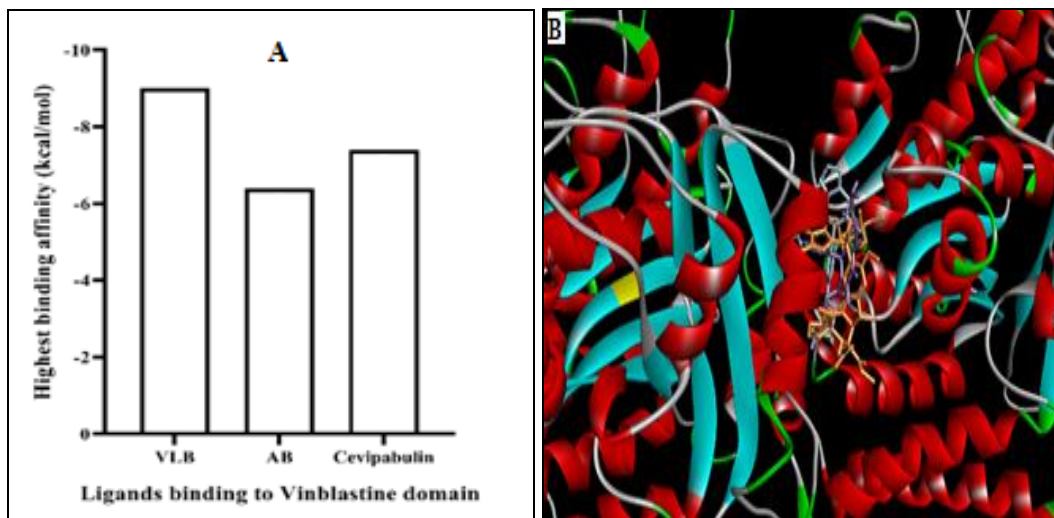


FIG. 3: BINDING AFFINITY AND BINDING SITE COMPARISON OF AMLODIPINE BESYLATE TO VINBLASTINE CRYSTAL VLB AND CEVIPABULIN TO THE VINBLASTINE BINDING SITE OF MODELLED TUBULIN-VINBLASTINE COMPLEX (PDB ID:1Z2B): A) OUR LIGAND HAS A BINDING AFFINITY OF -6.4 KCAL/MOL WHICH IS COMPARABLE TO THE POSITIVE CONTROL DRUG CEVIPABULIN THAT HAS A BINDING AFFINITY OF -7.4 KCAL/MOL AND THE REFERENCE DOCKED NATIVE LIGAND VLB SHOWS THE BINDING AFFINITY OF -9.0 KCAL/MOL. B) AMLODIPINE BESYLATE (PURPLE) HAS AN OVERLAPPING BINDING SITE TO CEVIPABULIN (GREY) AND REFERENCE CRYSTAL VINBLASTINE VLB (ORANGE) TO THE MODELLED TUBULIN-VINBLASTINE BINDING SITE OF CRYSTAL STRUCTURE 1Z2B WITH ALPHA AND BETA SUBUNITS

Hydrophobic interactions and hydrogen bonds act as an important contributor to the stability of proteins. The results showed that hydrogen bond, hydrophobic and other interactions are mediated by various amino acid residues obtained after

Docking. Similar key amino acid residues were found to be interacting with the native ligand of the crystal (VLB) **Fig. 4** and our desired drug ligand (Amlodipine besylate) as shown in **Table 3** and **Table 5**.

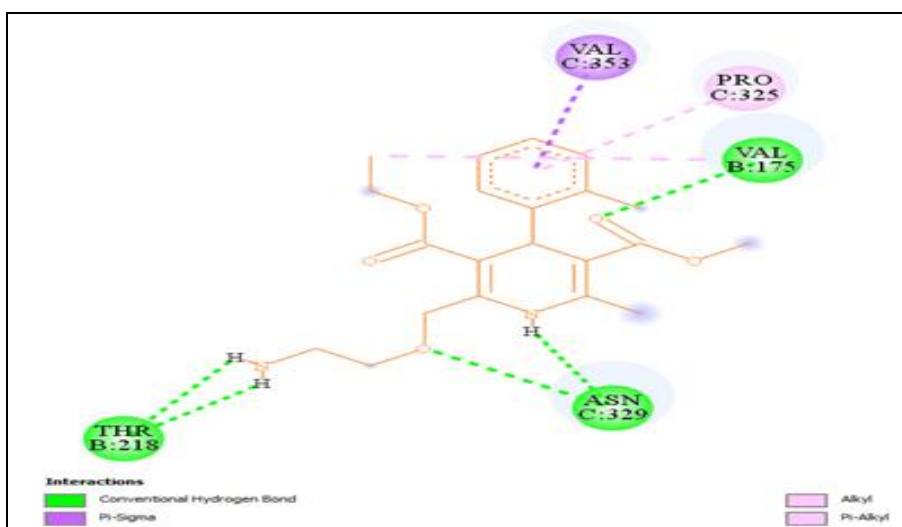


FIG. 4: RESIDUE LEVEL INTERACTION OF AMLODIPINE BESYLATE (1ST POSE) WITH MODELLED TUBULIN-VINBLASTINE COMPLEX (PDB ID: 1Z2B): UPON REMOVAL OF THE REFERENCE LIGAND (VLB) AND DOCKING OF THE LIGAND (ORANGE) TO ITS BINDING SITE SHOWED COMMON INTERACTING AMINO ACID RESIDUES WITH BOND DISTANCE AS MENTIONED IN TABLE 5. THE RESULT WAS OBTAINED FROM DOCKING BY AUTODOCK-VINA AND VISUALIZED BY DISCOVERY STUDIO BIOVIA 2020.

TABLE 5: THE INTERACTING RESIDUES OF THE MODELLED CRYSTAL STRUCTURE (PDB ID: 1Z2B) WITH THE DIHYDROPYRIDINE DERIVATIVE (AMLODIPINE BESYLATE) AND THE TYPE OF BONDS WITH RESPECTIVE DISTANCES OBTAINED FROM DOCKING BY AUTODOCK-VINA AND VISUALIZED BY DISCOVERY STUDIO BIOVIA 2020(B DENOTES β CHAIN AND C DENOTES α CHAIN). THE HIGHLIGHTED AMINO ACID RESIDUES CORRESPOND TO THE RESIDUES PRESENT IN THE BINDING POCKET THAT INTERACTS WITH THE NATIVE LIGAND VLB IN THE CRYSTAL STRUCTURE

Interacting residues	Bond type	Distance (Å)
C:ASN329	Hydrogen Bond	2.81
B:VAL175	Hydrogen Bond	2.51
C:ASN329	Hydrogen Bond	2.44
B:THR218	Hydrogen Bond	2.63
B:THR218	Hydrogen Bond	2.84
C:VAL353	Hydrophobic	3.96
B:VAL175	Hydrophobic	4.20
C:PRO325	Hydrophobic	5.16

Amlodipine besylate formed hydrophobic interactions with only two residues and one of them was the same amino acid residue that was involved in the binding of VLB with the tubulin crystal 1Z2B (VAL 353 of A chain) and out of the five hydrogen bonds, four hydrogen bonds with ASN 329 (C chain), THR 218 and VAL 175 (B chain) were found to be similar to VLB.

Three compounds derived from vinca alkaloid derivative 3'-cyanoanhydrovinblastine interacts with the vinca binding site of tubulin as determined by AutoDock Vina program and inhibits tubulin polymerization by interacting with the same amino acid residues as Amlodipine in the docked structure²².

Various experimental evidences have shown that vinca binding to the α subunit of tubulin and the hydrogen bond between vinca and ASN 329 and the hydrophobic interaction with VAL 353 of α -tubulin is crucial to consider a drug as a vinca binding site inhibitor²³.

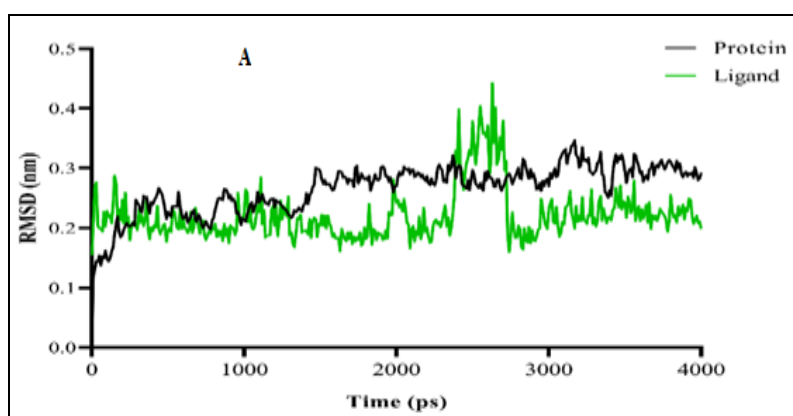
Thus, from the *in-silico* analysis we could speculate that this Dihydropyridine derivative may have the

potential to inhibit the polymerization of tubulin like vinblastine by binding to the protein tubulin. The data revealed a degree of similarity between the tubulin binding site of vinblastine and Amlodipine besylate.

MD Simulation Studies Revealed the Stability of the Highest Binding Affinity Complex Structure Obtained from Docking: Molecular dynamics simulation studies were done to understand the binding mode of Tubulin-Amlodipine besylate complex over a period of time. Parameters such as RMSD and Rg help in the understanding of this binding pattern.

The RMSD was calculated to examine the stability of the protein-ligand complex. The data revealed that the RMSD of the protein was 0.292Å **Fig. 5A** and the Tubulin-AB complex was well equilibrated and showed minimum deviation of 0.199Å till 4ns **Fig. 5A**.

The total potential energy, Coulomb energy and van der Waals of the modelled structure was found to be energetically stable during the simulation **Fig. 5B, C, D**.



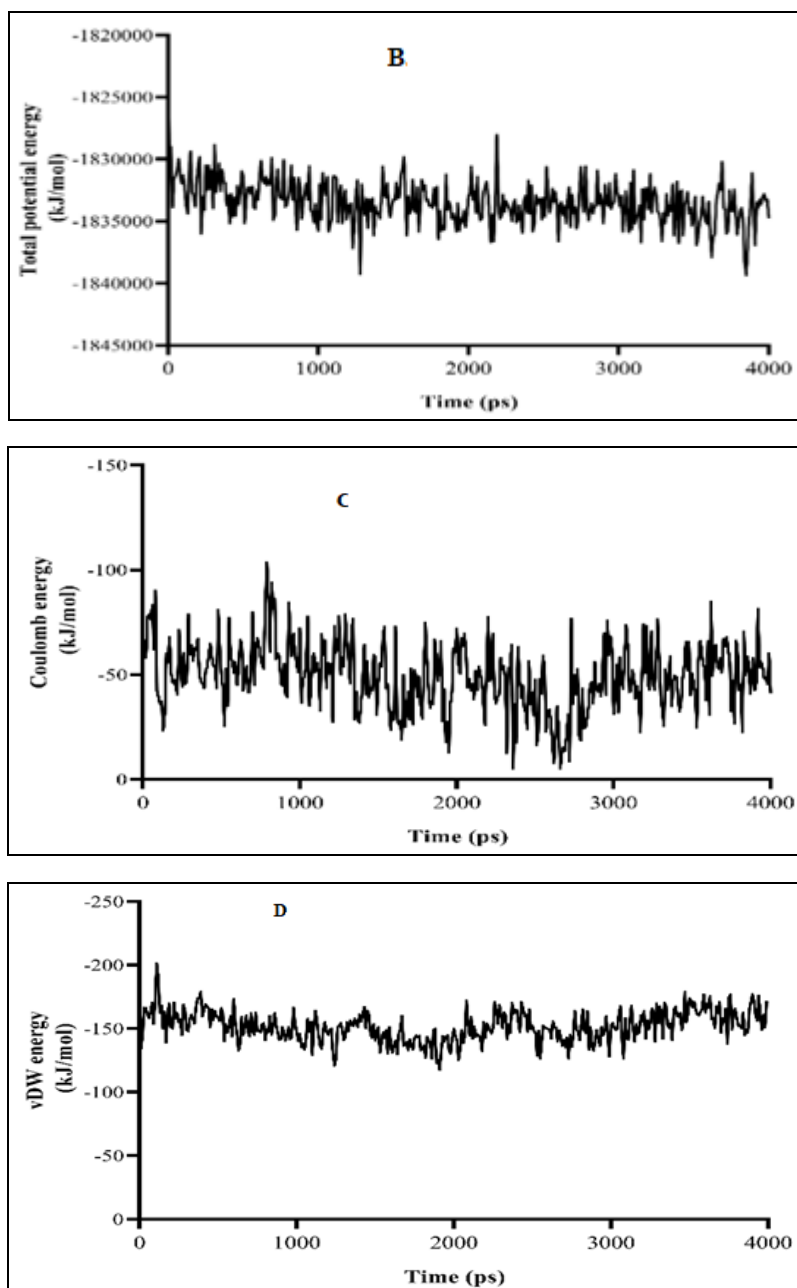


FIG. 5: PROTEIN STABILITY CORRESPONDING TO 4NS OF MD SIMULATION AT 300K A) RMSD OF TUBULIN PROTEIN AND OF TUBULIN-AB DOCKED COMPLEX B) POTENTIAL ENERGY GRAPH OF TUBULIN-AB DOCKED COMPLEX. C) COULOMB ENERGY GRAPH OF TUBULIN-AB DOCKED COMPLEX. D) VAN DER WAALS ENERGY GRAPH OF TUBULIN-AB DOCKED COMPLEX

Amlodipine Besylate Induced Cytotoxicity in HeLa/MCF-7/HCT-116/NKE Cells: In this study, we wanted to validate the *in-silico* data by *in-vitro* experiments using cancer cells. As the ligand showed its potential to act as a vinblastine binding site inhibitor via Docking, it was important to check whether Amlodipine besylate elicits cytotoxic effects on cancer cells without affecting the non-cancerous cells. By trypan blue dye exclusion method, this Dihydropyridine derivative showed potential anti-mitotic activity with greater

specificity towards cervical cancer cells (HeLa) than breast cancer cells (MCF-7), human colorectal cancer cells (HCT116) and not on non-cancerous normal cells (NKE) **Fig. 6.** The inhibitory concentration for 50 % of cells death (IC_{50}), was estimated at $10\mu M$ concentration for HeLa cells, $>10\mu M$ for MCF-7 cells, $>20\mu M$ for HCT116 cells and $20\mu M$ (twice the IC_{50} of cancer cell line) for non-cancerous cells. So, Amlodipine besylate showed greater specificity towards cervical cancer cells, which were chosen for further studies.

A compound known as Ansamitocin P3, that has been found to bind to the vinblastine site of tubulin, acts as a potent tubulin inhibitor and was shown to

inhibit cell proliferation in HeLa, MCF7 and MDA-MB-231 cells²⁴.

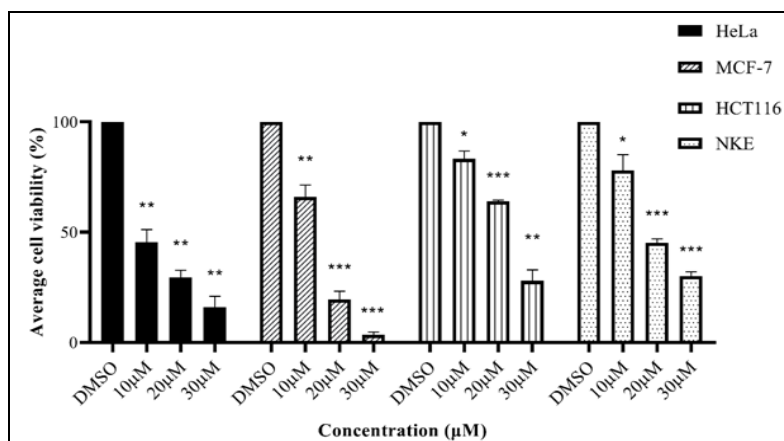


FIG. 6: CYTOTOXIC ACTIVITY OF AMLODIPINE BESYLATE IN THREE DIFFERENT CANCER CELL LINES INCLUDING HELA (CERVICAL CANCER), MCF-7 (BREAST CANCER) AND HCT116 (COLORECTAL CANCER) WERE COMPARED TO A NON-CANCEROUS NKE (NORMAL KIDNEY EPITHELIAL) CELLS. Cells were treated with different concentrations of amlodipine besylate for 24 h and cytotoxicity was measured using trypan blue exclusion method. As the drug is DMSO soluble so cells only treated with 0.05 % DMSO was used as control. (*P< 0.05, **P< 0.01 and ***P< 0.001).

Amlodipine Besylate Inhibits Migration of Cervical Cancer Cells: To ascertain the inhibitory effect of the drug on cervical cancer cell migration, scratch assay was performed using HeLa cells. The cells were treated with IC₅₀ value 10µM concentration for 0, 24 and 48 h, and a wound was introduced on the cells. Wound size in cells that

were not treated with Amlodipine besylate, gradually decreased with time whereas the relative change in the wound width of HeLa cells treated with the drug remained unaltered both at both 24 and 48 h **Fig. 7**. This suggests that the treatment with Amlodipine besylate inhibits cell migration.

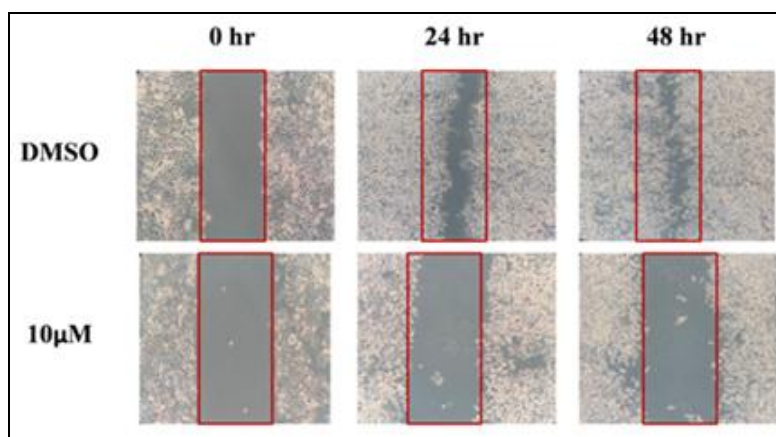


FIG. 7: AMLODIPINE BESYLATE INHIBITS HELA CELL MIGRATION IN A TIME-DEPENDENT MANNER. HELA CELLS WERE GROWN (80-90% CONFLUENT) AND A STERILE TIP INTRODUCED A WOUND. CELLS WERE TREATED IN TRIPPLICATE WITH OR WITHOUT THE DRUG (10 µM) FOR 24 AND 48 H. THE WOUND CLOSURE WAS OBSERVED AT THE INDICATED TIME PERIOD

Amlodipine Besylate Altered Microtubule Architecture in HeLa Cells: To illustrate whether the drug Amlodipine besylate caused any structural changes in microtubule and altered cell morphology, cultured HeLa cells were treated with

various concentrations of the drug (5 µM, 10µM and 20µM) for 24hours. Visualizing the cells under confocal microscope showed morphological changes in the microtubule network, which was disrupted in HeLa cells treated with different drug

concentrations compared to cells treated with vehicle only as control (0.05% DMSO) that displayed normal microtubule organization **Fig. 8**. The effect was more drastic in cells treated with 10 μ M (IC₅₀) and 20 μ M (2IC₅₀) of the drug. The cells became more round-shaped, suggesting some detachment from the substratum. There was cell shrinkage and contraction of cytoskeleton.

Disruptions in normal cell morphology originated probably from the result of the disruption of microtubules as they were treated with AB that affected cytoskeleton integrity and cell shape. This result is supported by previous reports where it was observed that the compound G-1 inhibits breast cancer cell growth by affecting microtubule assembly and altering its cellular morphology²⁵.

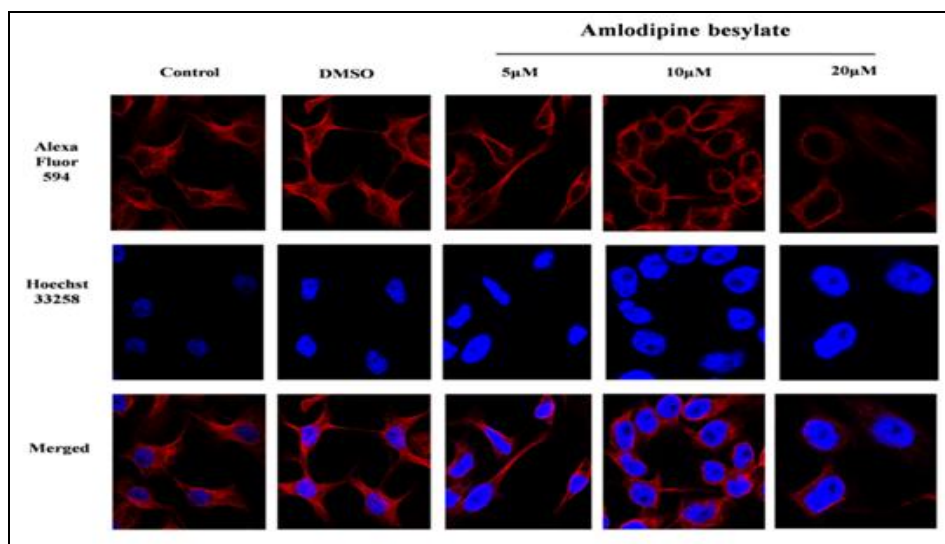


FIG. 8: AMLODIPINE BESYLATE ALTERS THE MICROTUBULE STRUCTURE IN A DOSE-DEPENDENT MANNER. HELA CELLS WERE LEFT UNTREATED OR TREATED WITH DIFFERENT CONCENTRATIONS OF AMLODIPINE BESYLATE FOR 24 H AND THE MICROTUBULE NETWORK WAS STAINED BY ANTI-A-TUBULIN ANTIBODY FOLLOWED BY STAINING WITH ALEXA-594-LABELED ANTI-MOUSE IGG ANTIBODY (RED FLUORESCENCE) AND VISUALIZED BY CONFOCAL MICROSCOPY. THE NUCLEUS WAS STAINED WITH HOECHST 33258 (BLUE FLUORESCENCE)

Amlodipine Besylate Depolymerized Microtubules in HeLa cells: To confirm whether Amlodipine besylate induces microtubule

depolymerization in HeLa cells, the ratio of polymeric to total tubulin in HeLa cells was determined by western blotting **Fig. 9A**.

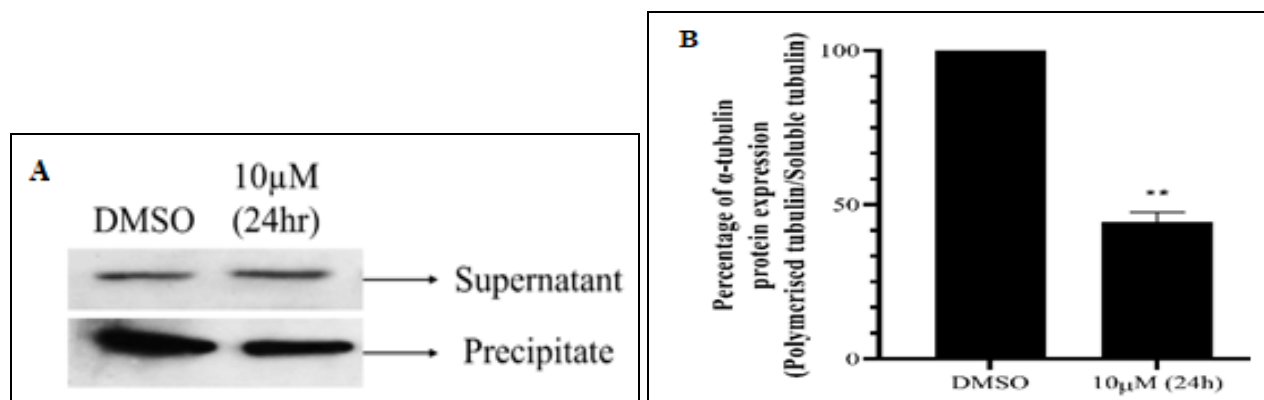


FIG. 9: AMLODIPINE BESYLATE REDUCES THE PRECIPITATE (POLYMERIC)/SOLUBLE TUBULIN FRACTION IN HELA CELLS. a) HeLa cells were treated with 10 μ M concentration of Amlodipine besylate for 24h. The polymerized fraction and the free fraction of tubulin were separated by centrifugation and was further processed by western blotting using monoclonal antibody against α -tubulin. Three independent experiments were carried out and a representative blot is shown. b) Percentage of polymerized/soluble α -tubulin protein expression was determined in HeLa cells after treatment with Amlodipine besylate. The quantification was done using ImageJ software and student's t-test was used to determine the statistical significance (**P<0.01).

The ratio was determined in the absence and presence of the drug for 24 h. The decrease in the polymeric tubulin and the increase in the soluble fraction indicates the extent of depolymerization of the microtubules. A decrease in the polymeric tubulin and increase in the soluble fraction was observed at 10 μ M concentration of AB at 24h (56%) where DMSO (control) is represented as 100%. This suggests that Amlodipine besylate depolymerizes microtubules in HeLa cells **Fig. 9B** coinciding with the confocal microscopy data where we find an alteration in the microtubule architecture **Fig. 8**. various reports on tubulin depolymerization drugs such as structural analogues of Combretastatin A-4 showed strong disassembly of cellular microtubules in HeLa cells²⁶.

CONCLUSION: The results from our present study collectively suggest that Amlodipine besylate might act as a potential tubulin inhibitor by binding to the vinblastine site. Amlodipine shows cytotoxic effects and inhibition of migration on cervical cancer cells probably by altering the microtubule architecture and thus disrupting the cytoskeletal integrity. Thus, Amlodipine besylate which effectively acts as a microtubule targeting agent could be a potential candidate for future anti-cancer drug development.

ACKNOWLEDGEMENTS: Sampurna Bhattacharya acknowledges University of Calcutta for her University Research Fellowship (DPO/51/F2183). We express our gratitude to Dr. Mahadeb Pal of Bose institute, Kolkata for providing the cells required for our experiments. We would like to thank Dr. Soumalee Basu of Calcutta University for helping us with the *in-silico* study analysis.

Declarations:

Ethics Approval and Consent to Participate: Nil

Availability of Data and Materials: The data supporting this study's findings are available from the corresponding author upon request.

Competing Interests: The authors declare no competing interests.

Funding: The DST-TARE grant supported the work (EMR/TAR/2018/000336).

CONFLICT OF INTEREST:

Ethics Approval and Consent to Participate: Nil

Availability of Data and Materials: The data supporting this study's findings are available from the corresponding author upon request.

Competing Interests: The authors declare no competing interests.

Funding: The DST-TARE grant supported the work (EMR/TAR/2018/000336).

Authors' Contributions: RS and SB conceptualized the *in-silico* study. RS and SG conceptualized the *in-vitro* study and are the corresponding authors of this manuscript. AL performed the MD simulation study. SB performed the research. RS, SG, AL and SB analyzed the data and wrote the paper. RS, SG, AL and SB have read and approved the final manuscript.

REFERENCES:

1. Cha Y, Erez T, Reynolds JJ, Kumar D, Ross J, Koytiger G, Kusko R, Zeskind B, Risso S, Kagan E and Papapetropoulos S: Drug repurposing from the perspective of pharmaceutical companies. *British Journal of Pharmacology* 2018; 175(2): 168-80.
2. Siddiqui S, Deshmukh AJ, Mudaliar P, Nalawade AJ, Iyer, D & Aich J: Drug repurposing: re-inventing therapies for cancer without re-entering the development pipeline a review. *Journal of the Egyptian National Cancer Institute*, 2022; 34(1): 1-12.
3. Subeha MR & Telleria CM: The anti-cancer properties of the HIV protease inhibitor nelfinavir. *Cancers* 2020; 12(11): 3437.
4. Blagosklonny MV: Cancer prevention with rapamycin. *Oncotarget* 2023; 14: 342.
5. Sung H, Ferlay J, Siegel RL, Laversanne M, Soerjomataram I, Jemal A & Bray F: Global cancer statistics 2020: GLOBOCAN estimates of incidence and mortality worldwide for 36 cancers in 185 countries. *CA: a Cancer Journal for Clinicians* 2021; 71(3): 209-249.
6. Wang X, Zhang H and Chen X: Drug resistance and combating drug resistance in cancer. *Cancer Drug Resistance* 2019; 2(2): 141-60.
7. Lafanechère L: The microtubule cytoskeleton: An old validated target for novel therapeutic drugs. *Frontiers in Pharmacology* 2022; 3888.
8. Garcin C & Straube A: Microtubules in cell migration. *Essays in Biochemistry* 2019; 63(5): 509-520.
9. Coulup SK and Georg GI: Revisiting microtubule targeting agents: α -Tubulin and the pironetin binding site as unexplored targets for cancer therapeutics. *Bioorganic & Medicinal Chemistry Letters* 2019; 29(15): 1865-73.
10. Field JJ, Kanakkanthara A and Miller JH: Microtubule-targeting agents are clinically successful due to both mitotic and interphase impairment of microtubule

- function. *Bioorganic & Medicinal Chemistry* 2014; 22(18): 5050-9.
11. Verma V, Sharma S, Gaur K & Kumar N: Role of vinca alkaloids and their derivatives in cancer therapy 2022.
 12. Dhyani P, Quispe C, Sharma E, Bahukhandi A, Sati P, Attri DC & Cho WC: Anticancer potential of alkaloids: a key emphasis to colchicine, vinblastine, vincristine, vindesine, vinorelbine and vincamine. *Cancer Cell International* 2022; 22(1): 1-20.
 13. Chengyong W, Jinghong X, Yanyan W, Qing-Jie X, Lingling M, Yuyan L & Yuxi W: The high-resolution X-ray structure of vinca-domain inhibitors of microtubules provides a rational approach for drug design. *FEBS Letters* 2021; 595(2): 195-205.
 14. Mishra AP, Bajpai A & Rai AK: 1, 4-Dihydropyridine: a dependable heterocyclic ring with the promising and the most anticipable therapeutic effects. *Mini Reviews in Medicinal Chemistry* 2019; 19(15): 1219-1254.
 15. Sheraz MA, Ahsan SF, Khan MF, Ahmed S and Ahmad I: Formulations of amlodipine: a review. *Journal of Pharmaceutics* 2016; 2016.
 16. Goto RN, Sobral LM, Sousa LO, Garcia CB, Lopes NP, Marin-Prida J, Ochoa-Rodriguez E, Verdecia-Reyes Y, Pardo-Andreu GL, Curti C and Leopoldino AM: Anticancer activity of a new dihydropyridine derivative, VdIE-2N, in head and neck squamous cell carcinoma. *European Journal of Pharmacology* 2018; 819: 198-206.
 17. Pan X, Li R, Guo H, Zhang W, Xu X, Chen X and Ding L: Dihydropyridine calcium channel blockers suppress the transcription of PD-L1 by Inhibiting the Activation of STAT1. *Frontiers in Pharmacology* 2021; 11: 2233.
 18. Trott O and Olson AJ: Software news and update autodock vina: improving the speed and accuracy of Docking with a new scoring function. *Efficient Optimization and Multithreading* 2009.
 19. Ye Q, Liu K, Shen Q, Li Q, Hao J, Han F & Jiang RW: Reversal of multidrug resistance in cancer by multi-functional flavonoids. *Frontiers in Oncology* 2019; 9: 487.
 20. Ayral-Kaloustian S, Zhang N and Beyer C: Cevipabulin (TTI-237): preclinical and clinical results for a novel antimicrotubule agent. *Methods and Findings in Experimental and Clinical Pharmacology* 2009; 31(7): 443-7.
 21. Yang J, Yu Y, Li Y, Yan W, Ye H, Niu L, Tang M, Wang Z, Yang Z, Pei H and Wei H: Cevipabulin-tubulin complex reveals a novel agent binding site on α -tubulin with tubulin degradation effect. *Science Advances* 2021; 7(21): eabg4168.
 22. Quan PM, Binh VN, Ngan VT, Trung NT and Anh NQ: Molecular docking studies of Vinca alkaloid derivatives on Tubulin. *Vietnam J of Chemistry* 2019; 57(6): 702-6.
 23. Venghateri JB, Gupta TK, Verma PJ, Kunwar A and Panda D: Ansamitocin P3 depolymerizes microtubules and induces apoptosis by binding to tubulin at the vinblastine site. *PLoS one* 2013; 8(10): 75182.
 24. Lv X, He C, Huang C, Hua G, Wang Z, Remmenga SW & Wang C: G-1 inhibits breast cancer cell growth via targeting colchicine-binding site of tubulin to interfere with microtubule assembly. *Molecular Cancer Therapeutics* 2017; 16(6): 1080-1091.
 25. Hura N, Sawant AV, Kumari A, Guchhait SK and Panda D: Combretastatin-inspired heterocycles as antitubulin anticancer agents. *ACS Omega* 2018; 3(8): 9754-69.
 26. Vincent ZACM, Aurélien G, Olivier M and SwissParam: A fast force field generation tool for small 150 organic molecules. *J Comput Chem* 32: 2359-68.
 27. Jorgensen WL, Chandrasekhar J, Madura JD, Impey RW & Klein ML: Comparison of simple potential functions for simulating liquid water. *The Journal of Chemical Physics* 1998; 79(2): 926. <https://doi.org/10.1063/1.445869>
 28. Darden T, York D & Pedersen L: Particle mesh Ewald: An N \cdot log(N) method for Ewald sums in large systems. *The Journal of Chemical Physics* 1993; 98(12): 10089. <https://doi.org/10.1063/1.464397>

How to cite this article:

Bhattacharya S, Lahiri A, Gupta S and Sur R: Identifying tubulin as a new target of a dihydropyridine derivative, amlodipine besylate. *Int J Pharm Sci & Res* 2023; 14(12): 5687-00. doi: 10.13040/IJPSR.0975-8232.14(12).5687-00.

All © 2023 are reserved by International Journal of Pharmaceutical Sciences and Research. This Journal licensed under a Creative Commons Attribution-NonCommercial-ShareAlike 3.0 Unported License.

This article can be downloaded to **Android OS** based mobile. Scan QR Code using Code/Bar Scanner from your mobile. (Scanners are available on Google Playstore)